Syndiotactic Polystyrene Intercalates from Naphthalene Derivatives

Sudip Malik,[†] Cyrille Rochas,[‡] Marc Schmutz,[†] and Jean Michel Guenet*,[†]

Institut Charles Sadron, CNRS UPR 22, 6 rue Boussingault, BP 40016, F-67083 Strasbourg Cedex, France, and Laboratoire de Spectrométrie Physique CNRS−UJF UMR5588, 38402 Saint Martin d'Hères Cedex, France

Received April 14, 2005

ABSTRACT: The formation of syndiotactic polystyrene (sPS) intercalates in a series of solvent derived from naphthalene, namely naphthalene, 1,2,3,4-tetrahydro naphthalene (tetralin), and *trans*-decahydronaphthalene (*trans*-decalin) has been investigated. For each systems, the temperature−concentration phase diagrams have been established by DSC, the morphology has been observed by optical and electron microscopy, and the molecular structure has been determined by time-resolved X-ray diffraction and neutron diffraction. The morphology depends on the solvent used: in naphthalene and tetralin fibrillar arrays are observed as opposed to assemblies of spherulites in *trans*-decalin. This morphology might be related to the nature of the intercalates formed: *congruently melting* in naphthalene and tetralin; *incongruently melting* in *trans*-decalin. The time-resolved X-ray and the neutron diffraction investigations are in agreement with the outcomes from the temperature−concentration phase diagrams.

Introduction

Since its recent synthesis syndiotactic polystyrene (sPS) has been receiving continuous interest thanks to its high crystallization rate and high melting temperature[1−3] which makes it a polymer for potential industrial applications. sPS crystallizes into several crystalline modifications with chains in either a planar zigzag or helical conformation. Two crystalline forms, α and β consist of an all-trans planar zigzag conformation and two forms, δ and γ are made up with chains under a 2_1 helical conformation.[4−7] While the α and β forms can be grown from the bulk state, the δ and γ forms are only produced in the presence of solvent molecules.[4] The δ form has been shown to consist of polymer−solvent intercalates (also designated as polymer−solvent compounds, crystallosolvates, or chlathrates) where polymer chains and solvent molecules are intimately organized.[7,8] The γ form is produced after desolvation of the δ form. sPS has the propensity to form intercalates with a large variety of solvents of disparate chemical structures such as benzene,[9] toluene,[10] chloroform,[10,11] bromoform,[12] and diethylbenzene,[13] while the diffraction pattern of the δ form is basically the same. Solvent intercalation is achieved either by exposing solid polymer to liquid solvent or vapor (solvent-induced process)[4,5,14−15] or by cooling homogeneous solution (solution-cast process).[8−12] The purpose of this paper is to gain further knowledge on the formation of sPS intercalates by examining the effect of small modifications of solvent structure on the nature of these systems. In this aim, we have selected three solvents from the naphthalene series, namely naphthalene (below, left), 1,2,3,4-tetrahydronaphthalene (below, middle) and decahydronaphthalene (below, right).

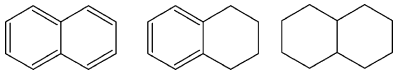

While in the three cases the structure consists of two concatenated rings, the partial and total protonation of the double bonds is likely to introduce some modifications on compound formation. In this paper, we shall report on the temperature−concentration phase diagrams, the morphology, and the structure as observed by time-resolved X-ray and neutron diffraction as well as by small-angle neutron scattering.

* Corresponding author. E-mail: guenet@ics.u-strasbg.fr. Web: http://www-ics.u-strasbg.fr/perso/jmg/guenet.php. Telephone: +33 (0) 388 41 40 87. Fax: +33 (0) 388 41 40 99.
[†] Institut Charles Sadron.
[‡] Laboratoire de Spectrométrie Physique CNRS−UJF UMR5588.

Experimental Section

1. Materials. The syndiotactic polystyrene (sPS) samples, either hydrogeneous (sPSH) or deuterated (sPSD), were synthesized by using a method devised by Zambelli and coworkers.[2] The content of syndiotactic triads as characterized by ^{1}H NMR was found to be over 99%. The molecular weight characterization of these samples was performed by SEC in dichlorobenzene at 140 °C and yielded the following values: $M_w = 1.0 \times 10^5$ with $M_w/M_n = 4.4$ for sPSH; $M_w = 4.3 \times 10^4$ with $M_w/M_n = 3.6$ for sPSD.

Hydrogeneous and deuterated naphthalene, *trans*-decalin (*trans*-decahydronaphthalene), and tetralin (tetrahydronaphthalene) were purchased from Aldrich and were used without further purification. Deuterated *trans*-decalin was purchased from Eurisotop (Saclay, France).

2. Techniques. Optical Microscopy. Optical investigations by means of Nomarsky phase contrast were carried out with a NIKON Optiphot-2 equipped with a CCD camera. Image processing and analysis were achieved by means of LUCIA, a software developed by Laboratory Imaging. The samples used for optical observation were prepared by remelting between glass slides those samples prepared beforehand in a test tube. To minimize solvent evaporation the edge of the thin upper glass slide was glued with epoxy resin.

Transmission Electron Microscopy. Gels were sandwiched between two copper specimen holders and rapidly frozen in liquid nitrogen, to keep the solvent in a glassy, amorphous state while preserving the inner structure of the gels. The frozen samples were then transferred onto the fracture-replication stage which was kept at $T = -162$ °C and under vacuum of $P = 5 \times 10^{-8}$ mbar. The shadowing with Pt/C was immediately performed after fracturing the sample, and a 2 nm layer was deposited under a 45° angle. The replica was reinforced with a 20 nm thick layer of carbon at 90°. The replicas were retrieved and cleaned in hot toluene and observed with a Philips CM12 microscope operating at 120 kV.

Scanning Electron Microscopy. A Hitachi S-2300 operating in a voltage range from 15 to 25 kV was used. A film of sPS/naphthalene system was dried in a vacuum at room

10.1021/ma050793f CCC: $30.25
Published on Web 06/10/2005

temperature, and then was coated in an argon atmosphere with a gold layer of thickness 40 nm by the usual sputtering technique.

Differential Scanning Calorimetry. The thermal behavior of these systems was investigated by means of Perkin-Elmer DSC 7. The systems once placed into hermetically sealed sample pans were systematically remelted above 200 °C for 10 min and then cooled to 20 °C or below at a rate of 5 °C/min. The thermograms were recorded at a heating rate of 5 °C/min. The weight of the sample pan was checked after each experiment and the instrument was calibrated with indium before each set of experiment.

Two procedures were employed for producing adequate DSC samples. The first procedure was typically used for polymer fractions lower than $X_{pol} = 0.30$ g/g. Homogeneous solutions were prepared by heating at desired temperature in hermetically closed test tube that contained a mixture of appropriate amount of polymer and solvent. Intercalates were obtained by a subsequent cooling of these solutions at room temperature. Pieces of the resulting samples were then transferred to "volatile sample" pan that were hermetically sealed.

Mixtures of polymer fractions higher than $X_{pol} = 0.30$ g/g were prepared by allowing evaporation of the solvent from low-concentrated sample (typically $X_{pol} = 0.30$ g/g) until the desired polymer fraction was reached as checked by weighing the sample. The samples were introduced into DSC pan which was hermetically sealed, and then subsequently heated to obtain a homogeneous system. To check the reliability of the second procedure, $X_{pol} = 0.35$ g/g sample was prepared by both procedures. No significant discrepancy was observed between either type of sample.

Kinetics effects that may occur on increasing polymer fraction, have been assessed by using different heating and cooling rates for a few samples representative of the different phases.

X-ray Diffraction. The X-ray experiments were performed on beamline BM2 at the European Synchrotron Radiation Facility (ESRF), Grenoble, France. The energy of the beam was 15.8 Kev which corresponds to a wavelength of $\lambda = 7.86 \times 10^{-2}$ nm. At the sample position the collimated beam was focused with a typical cross section of 0.1×0.3 mm^2. The scattered photons were collected onto a two-dimensional CCD detector developed by Princeton Instruments, presently Roper Scientific. Typical acquisition times were of about 20 s which allows time-resolved experiments to be carried out at an average rate of 2 °C/mn, a value close to the 5 °C/mn heating rate used for DSC experiments. Note that, however, that the heating procedure is stepwise unlike that in DSC experiments.

The sample-to-detector distance was about 0.2 m, corresponding to a momentum transfer vector q range of $1 < q$ (nm^{-1}) < 17, with $q = (4\pi/\lambda) \sin(\theta/2)$, where λ and θ are the wavelength and the scattering angle, respectively (further information is available on the following website http://www.esrf.fr).

The scattering intensities obtained were corrected for the detector response, the dark current, the empty cell, the sample transmission, and the sample thickness. To obtain a one-dimensional X-ray pattern out of the two-dimensional digitalized pictures, the data were radially regrouped, and a silver behonate sample was used for determining the actual values of the momenta transfer q.

Samples were prepared in thin-wall glass tube (wall thickness $\approx$ 1 mm) and of 4 cm height. Approximately 300 mg of sample was then produced which allows homogeneous systems to be obtained directly into the glass tube, and therefore bypass a sample transfer procedure. As a matter of fact, rapid evaporation frequently occurs with small-sized samples when they are introduced into a classical X-ray measuring cell, an effect which is liable to skew the results in the case of polymer−solvent compounds.

Neutron Diffraction. Neutron diffraction can be an appropriate investigation tool for systems involving polymer−solvent compounds thanks to the deuterium-labeling possibility of either component.[16,17] When dealing with a binary system, four labeling possibilities are accessible, which provides one with four structure factors without significantly changing the molecular arrangement as illustrated by the general expression for the intensity diffracted by a binary system composed of one type of polymer and one type of solvent:

$$I(q) = A_p^2(q)S_p(q) + A_s^2(q)S_s(q) + 2A_p(q)A_s(q)S_{ps}(q) \quad (1a)$$

where $A(q)$ and $S(q)$ with appropriate subscripts are the coherent scattering amplitude and the structure factor of the polymer (p) and of the solvent (s), and $S_{ps}(q)$ is a cross term which is related to the co-organization of the polymer and the solvent. Changing the labeling of the solvent while keeping the polymer labeling the same generally results in an alteration of the ratio of the intensities of the diffraction peaks related to the compound. Conversely, if no complex is formed, this cross term vanishes so that the reflections arising from the crystallized polymer are independent of the solvent labeling.

Neutron diffraction experiments were carried out on D16, a two-circle diffractometer located at Institut Laue Langevin, Grenoble, France. This diffractometer is equipped with a position sensitive ^{3}He multidetector with 128×128 wires. It operates at a wavelength $\lambda = 0.454$ nm obtained by diffraction of the neutron beam onto a pyrolytic graphite mosaic crystal oriented under Bragg conditions (further details available at http://www.ill.fr). Momenta transfer $q = (4\pi/\lambda) \sin(\theta/2)$were ranging from $q = 2$ to 12 nm^{-1}. Detector calibration and correction for cell efficiency were achieved by means of a light water spectrum.

The intercalates were prepared directly in amorphous quartz tubes of 3 mm inner diameter. After introducing a mixture of polymer and solvent these tubes were sealed from atmosphere. Homogeneous solution were obtained by heating, and the crystalline compounds were then allow to grow by a quench to room temperature.

Small-Angle Neutron Scattering. The experiments were performed on the PAXE camera located at the Laboratoire Léon Brillouin (LLB, CEN Saclay, France). A wavelength of $\lambda_m = 0.6$ nm was used with a wavelength distribution characterized by a full width at half-maximum, $\Delta\lambda/\lambda$, of about 10%. Neutron detection and counting was achieved with a built-in two-dimensional sensitive detector composed of 64×64 cells (further details are available at http://www-llb.cea.fr). By varying the sample−detector distance the available q range was $0.1 < q$ (nm^{-1}) < 2.5 where $q = (4\pi/\lambda) \sin(\theta/2)$, θ being the scattering angle.

Samples were prepared directly in sealable quartz cells from HELLMA of optical paths of 1 mm. After introducing appropriate mixtures of the deuterated polymer, the hydrogenous polymer, and hydrogenous naphthalene, the system was heated to 200 °C to obtain a homogeneous solution prior to a rapid cooling at room temperature.

The samples were studied at 20 and 165 °C by using a special sample holder allowing heating to high temperature within ±2 °C.

The position sensitive detector was calibrated by means of light water, a purely incoherent scatterer. Under these conditions the absolute intensity, $I_A(q)$, is written as

$$I_A(q) = I_N(q)/K \quad (1b)$$

in which $I_N(q)$ is the intensity obtained after background subtraction, transmission corrections and detector normalization, and K is a constant which reads

$$K = \frac{4\pi(a_D - a_H)^2\delta_w T_w N_A}{g(\lambda_m)(1 - T_w)m_i^2} \quad (2)$$

in which a_D and a_H are the coherent scattering amplitude of the deuterated polymer and the hydrogenous polymer, respectively, δ_w and T_w the thickness and the transmission of the calibration water sample, m_i the molecular weight of the

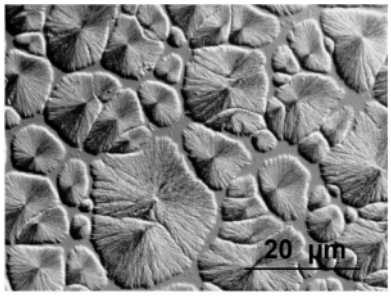

Figure 1. Spherulitic morphology of sPS/*trans*-decalin systems ($X_{pol} = 0.10$ g/g) as observed by Nomarsky phase contrast.

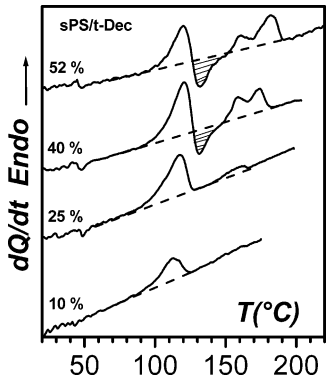

Figure 2. Typical DSC traces for sPS/*trans*-decalin system at indicated polymer concentration. Hatched areas highlight the exothermic events.

scattering unit (monomer), and $g(\lambda_m)$ a constant which is camera-dependent and was measured by using Cotton's method.[18] Note that the scattering amplitude of hydrogenous polystyrene in hydrogenous naphthalene, $(a_H - a_{NapH})$ is virtually nought. The intensities are expressed in dimensionless units.

Results and Discussion

Before discussing the results for each polymer/solvent couple, some general molecular features that characterize solvated and nonsolvated structures need be presented. For results reported here, the crystalline structure of the different phases has been studied by X-ray diffraction either as a function of polymer fraction at a fixed temperature or by time-resolved experiments at increasing temperature with a rate of 2 °C/min. The different polymer fractions studied have been selected here on the basis of the outcomes of the temperature−concentration phase diagram. It is worth mentioning that the reflections at $q = 5.5$ nm^{-1} ($d = 1.13$ nm) and $q = 7.4$ nm^{-1} ($d = 0.85$ nm) are characteristic peaks for the δ form of sPS [4,7] (the solvated form made up with 2_1 helices) and the reflections at $q = 4.5$ nm^{-1} ($d = 1.42$ nm), 7.6 nm^{-1} ($d = 0.83$ nm), 8.6 nm^{-1} ($d = 0.73$ nm), 9.0 nm^{-1} ($d = 0.7$ nm) and 10.0 nm^{-1} ($d = 0.63$ nm) belong to β form of sPS (the nonsolvated form with totally extended chains, namely the planar zigzag form).

1. sPS/*trans*-Decalin. The morphology of these systems has been essentially observed by optical microscopy. As a matter of fact, a spherulitic morphology occurs with spherulite sizes averaging around 20 μm diameter (see Figure 1). This morphology is independent of polymer fraction.

Typical DSC traces obtained at 5 °C/min for this system for different polymer concentration are presented in Figure 2. As can be seen an endotherm occurs at $T = 125 \pm 5$ °C over the concentration range. In the range of concentration $0.4 \leq X_{pol} \leq 0.70$ the first endotherm is immediately followed by an exothermic event and eventually by another endotherm consisting of two peaks. Note that the occurrence of an exotherm reveals the presence of a metastable phase in this system. Also, the surface ratio between the two peaks of the final endotherm is independent of the heating rate which rather suggests the existence of two different species (most probably lamellae of differing thickness) rather than a recrystallization process.

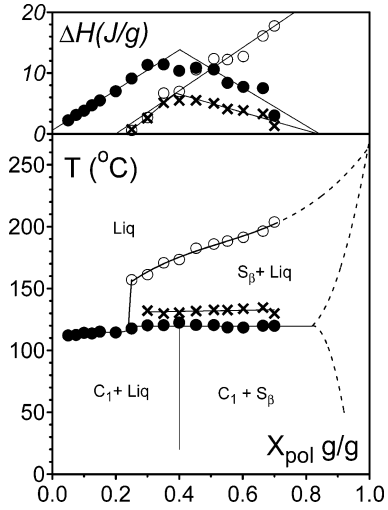

Figure 3. Temperature−concentration phase diagram and Tamman's diagram for sPS/*trans*-decalin systems. C_1 stands for a compound of stoichiometry 1/1 (molecules of solvent per monomer) and S_β stands for a solid polymer solution consisting of the nonsolvated planar zigzag structure.

In Figure 3, the temperatures related to each thermal event are plotted in order to establish the temperature−concentration phase diagram (T−C phase diagram). Also, the enthalpies corresponding to these thermal events are plotted in a Tamman's diagram in the same figure. Note that concerning the final endotherm only the temperature corresponding to the largest, final peak is reported. The results presented here are basically the same as those reported by Berghmans and Deberdt[19] except that the enthalpies of all the 1st-order thermal events are reported.

The T−C phase diagram clearly shows the existence of only one compound C_1 which turns out to be an incongruently melting compound. The incongruent melting takes place at $T = 125 \pm 5°$ through the temperature nonvariant event. As will be confirmed below by diffraction techniques, this compound consists of solvated 2_1 helical forms, namely the δ form. The enthalpy related to this temperature nonvariant endotherm increases linearly up to a polymer fraction X_c and then decreases linearly. The intersect of these two straight lines yields the stoichiometric composition of the compound, which provides one with a stoichiometry of about *one trans-decalin molecule per monomer*. Above $T = 125 \pm 5$ °C the compound transforms into a solid phase, namely S_β which consists of the *β form* of sPS as will be confirmed below (the composition of this phase $X_\beta = 0.84 \pm 0.02$ indicates that solvent molecules are trapped within the amorphous domains of this phase). Interestingly, the enthalpies associated with the $T = 125$ °C endotherm and with the acompanying exotherm both display a maximum at the stoichiometric composition. Also, they give the same composition $X_\beta = 0.84 \pm 0.02$ for the solid solution S_β at $T = 125$ °C. These outcomes

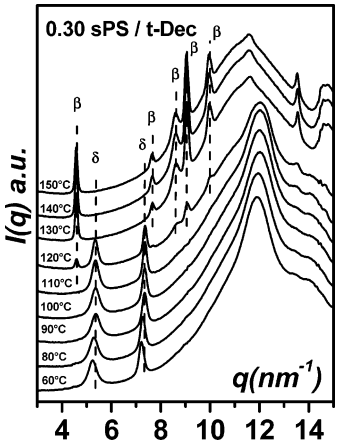

Figure 4. X-ray diffraction patterns of sPS/*trans*-decalin systems at $X_{pol} = 0.30$ g/g with acquisition times of 10 s and a heating rate of 2 °C/min. The main reflections of the δ form and the β form are shown.

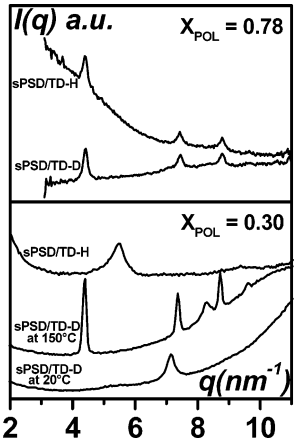

Figure 5. Neutron diffraction patterns for sPS/*trans*-decalin systems for different isotopic labeling: sPSD/*trans*-decalinD and sPSD/*trans*-decalinH. Key: upper figure, $X_{pol} = 0.78$ g/g; lower figure, $X_{pol} = 0.30$ g/g.

clearly indicate that the two events are intimately related. We suspect that the endothermic event at $T = 125 \pm 5$ °C corresponds to a total desolvation of the δ form, leaving nonsolvated 2_1 helices. It is known that these helices are not stable in the absence of solvent, so that the exotherm may well correspond to the transformation of these 2_1 helices into the planar zigzag form, which is stable. This further suggests that total desolvation of the 2_1 helices should produce an exotherm when incongruently melting compounds are dealt with. If partial desolvation occurs, then the 2_1 helices are likely to be still stable, so that no exotherm should be observed as has been already suggested by one of us.[20]

In Figure 4, X-ray diffractograms of sPS/*trans*-decalin system at a polymer fraction $X_{pol} = 0.30$ g/g are presented as a function of temperature. The typical reflections at $q = 5.5$ and 7.4 nm^{-1} of the δ form of sPS are present up to $T = 120$ °C while above $T = 120$ °C the reflections at $q = 4.5$, 7.6, 8.6, 9.0, and 10.0 nm^{-1} arising from the β form appear. This transition from one crystalline form into the other was expected from the phase diagram. Yet, the present experiments have not detected the metastable state giving rise to the exotherm arount $T = 130$ °C. This metastable state could be either an emptied chlathrate form, in which case there is no way to distinguish it from the δ form, or the so-called γ form. If the metastable state was the γ form, failure to detect it may be due to the physical limitation of the data acquisition procedure which takes about 20 s.

Neutron diffraction experiments are presented in Figure 5 for samples with differing deuterium-labeled species, and for different polymer fraction X_{pol}. At $X_{pol} = 0.3$ (w/w), the intensity ratio does vary with the solvent labeling. In sPSD/*trans*-decalin-*h* at room temperature, namely when the δ form is present, the peaks are labeling-dependent, in particular the ratio between the peak at $q = 5.5$ nm^{-1} and that at $q = 7.4$ nm^{-1} varies markedly whether one uses hydrogeneous or deuterated *trans*-decalin. Once the system is heated above 150 °C, the reflections at $q = 4.5$, 7.6, 8.6, 9.0, and 10.0 nm^{-1} appear in agreement with the phase diagram as well as with X-ray diffraction data. Similarly, experiments carried out at $X_{pol} = 0.73$ (w/w), namely in a concentration range where the δ form is virtually absent, and the β form is predominant, the diffraction patterns are not at all labeling-dependent as far as peak intensities are concerned. This shows that neutron diffraction together with isotopic labeling is a powerful and reliable technique for detecting qualitatively the presence of polymer−solvent compound.

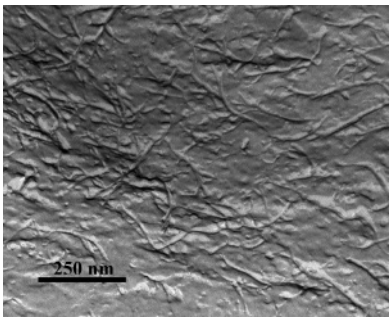

Figure 6. Transmission electron micrograph of sPS/tetralin system. Fibrils show up with an average diameter of about 8−14 nm.

2. sPS/Tetralin. In sPS/tetraline systems, the morphology as seen by electron microscopy on freeze-fractured samples is definitely fibrillar in a large range of polymer concentrations (see Figure 6). Fibrils cross-section diameters are ranging between 5 and 14 nm as indicated by image processing. As will be seen in what follows, fibrils are thinner than in sPS/naphthalene systems.

Typical DSC traces obtained at 5 °C/min for different polymer fraction X_{pol} of sPS/tetralin systems are shown in Figure 7. Unlike *trans*-decalin, no exotherm is observed. The temperature associated with the first endothermic event initially increases with increasing polymer fraction, goes through a maximum, and then decreases. The T−C phase diagram of sPS/tetralin drawn in Figure 8 suggests the occurrence of either a congruently melting or a singular-melting compound (C_1) whose stoichiometry is about *one tetralin molecule per monomer* as derived from the maximum of the enthalpy variation vs polymer fraction. (note that a singular-melting compound is the limiting case of a congruently melting compound). As will be shown below this compound correspond to the δ form. Here, the absence of an exotherm most probably arises from the congruently melting character of the compound, which transforms directly into a thermodynamically stable liquid at this temperature. Increasing the polymer fraction further eventually gives a solid-phase S_β which

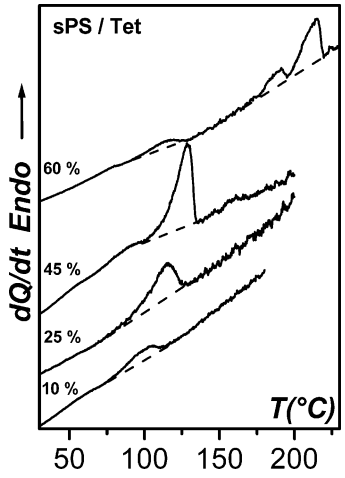

Figure 7. Typical DSC traces for sPS/tetralin system at indicated polymer fractions.

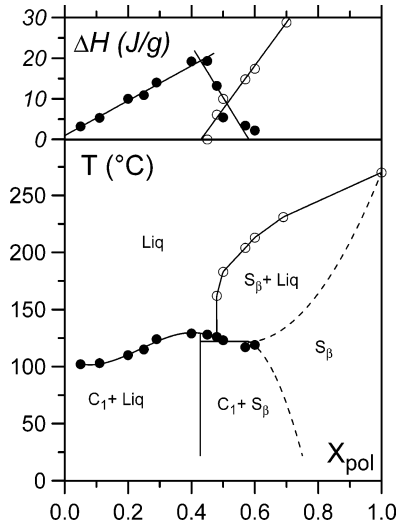

Figure 8. Temperature−concentration phase diagram and Tamman's diagram for sPS/tetralin system. C_1 stands for a compound of stoichiometry 1/1 (molecules of solvent per monomer) and S_β stands for a solid polymer solution consisting of the nonsolvated planar zigzag structure.

consists of the sPS β form. It is worth stressing that the composition $X_\beta = 0.68 \pm 0.02$ of the solid-phase S(β) is slightly less concentrated than that in *trans*-decalin. As with *trans*-decalin, only one compound occurs.

In Figure 9 are presented as a function of temperature X-ray diffractograms of sPS/tetralin systems at $X_{pol} = 0.40$ g/g and $X_{pol} = 0.48$ w/w, polymer fractions that are on either side of the stoichiomeric composition of the complex. At $X_{pol} = 0.40$ w/w, the reflections at $q = 5.5$ and 7.4 nm^{-1} of the δ form of sPS are seen in the entire temperature range as expected from the phase diagram. At $X_{pol} = 0.48$ w/w, the reflections at $q = 5.5$ and 7.4 nm^{-1} of the δ form are present up to $T = 140$ °Cwhile, above $T = 140$ °C, the reflections at $q = 4.5$, 7.6, 8.6, 9.0, and 10.0 nm^{-1} characteristic of the β form replace those due to the δ form, thus confirming the outcomes from the T−C phase diagram.

Because of nonavailability of deuterated tetralin, the same type of investigations as made with *trans*-decalin could not be carried out.

3. sPS/Naphthalene. Results on sPS/naphthalene systems have been already detailed in a previous paper.[21] We give here a brief summary for the sake of comparison with *trans*-decalin and tetralin. Unlike

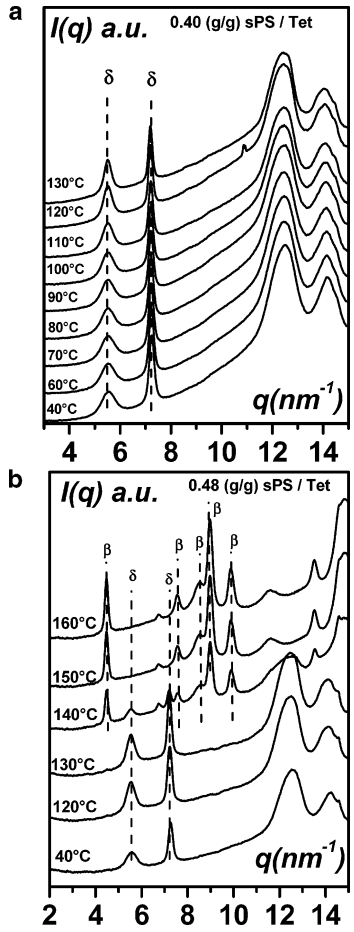

Figure 9. (a) X-ray diffraction patterns of sPS/tetralin intercalate at $X_{pol} = 0.40$ g/g (b) X-ray diffraction patterns of sPS/tetralin intercalate at $X_{pol} = 0.48$ g/g. In all cases, acquisition times of 10 s and heating rate of 2 °C/min were used. The main reflections of the δ form and the β form are shown.

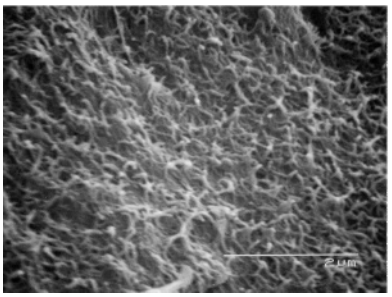

Figure 10. Scanning electron micrograph of sPS−naphthalene dried gels $X_{pol} = 0.25$ g/g. Fibrils cross-section diameters are somewhere between 40 and 95 nm.

trans-decalin and tetralin, which are liquid at room temperature, naphthalene is solid. The morphology of sPS/naphthalene systems is rather fibrillar as shown in Figure 10. Fibrils cross-section diameters are ranging from 30 to 95 nm as revealed by image processing. They are much thicker than those observed in sPS/tetralin systems.

Two temperature domains can be identified on DSC thermograms: a low temperature region, typically near 82 °C, where the melting endotherms are related to the only naphthalene, and a high-temperature region dealing with thermal events related to the polymer structures (Figure 11). Here it is also worth noticing that the naphthalene melting consists of two endotherms in the

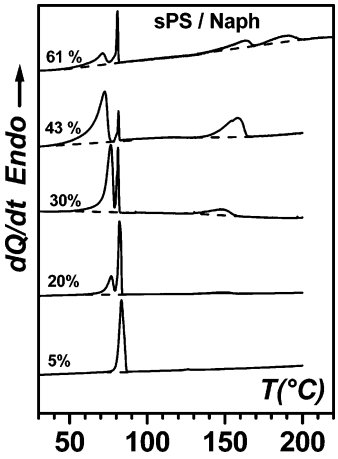

Figure 11. Typical DSC traces of sPS/naphthalene systems at indicated polymer fractions.

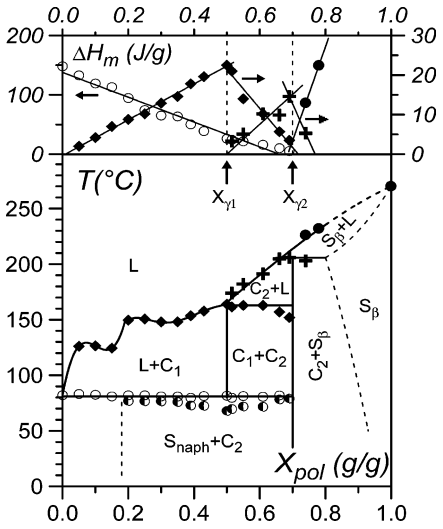

Figure 12. Temperature−concentration phase diagram and Tamman's diagram for sPS/naphthalene systems. C_1 and C_2 stand for two different compounds of stoichiometries 4/5 and 1/3 (molecules of solvent per monomer), respectively. $X_{\gamma 1}$ and $X_{\gamma 2}$ correspond to the stoichiometric compositions of compound C_1 and compound C_2, respectively. S_β stands for a solid polymer solution consisting of the nonsolvated planar zigzag structure.

temperature range 82−68 °C for polymer fractions above $X_{pol} > 0.20$ g/g. The origin of this behavior arises from the fact that increasing polymer fraction creates smaller and smaller free solvent crystals and according to Gibb's theory these finite-size crystals must display a melting point lower than that of infinite crystals.

The T−C phase diagram drawn in Figure 12 reveals the existence of the two compounds C_1 and C_2 of differing stoichiometries. C_1 is a singularly melting compound, while C_2 is an incongruently melting compound, yet very close to a singular-melting compound. Interestingly, C_1 transforms into compound C_2 in two ways: by heating above 160 °C in the range $0.5 < X_{pol} < 0.7$, and by cooling at low temperature, after naphthalene has crystallized in a polymer fraction range $0 < X_{pol} < 0.5$. From the Tamman diagram, the stoichiometry of the compound C_1 is about *four naphthalene molecules per five monomer units*, while the stoichiometry of compound C_2 is about *one naphthalene molecules per three monomer units*. This stoichiometry is slightly larger than that reported by Chatani and coworkers[7] for sPS-toluene system (*one toluene molecule per four monomer units*).

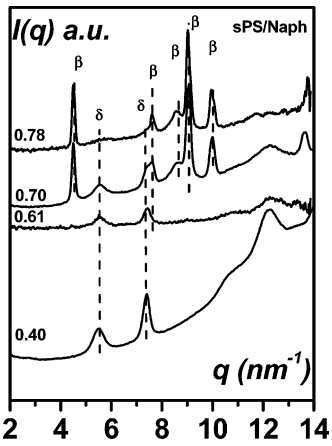

Figure 13. X-ray diffraction patterns of sPS/naphthalene systems at the indicated polymer fractions. Acquisition times of 10 s and heating rate of 2 °C/min were used. The main reflections of the δ form and the β form are shown.

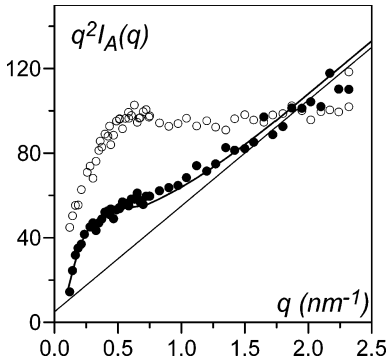

Figure 14. Scattering curve plotted by means of a Kratky representation ($q^2 I_A(q)$ vs q) for sPS_D chains ($\mathbf{C} = 0.06$ g/cm^3) in a 20% system ($X_{pol} = 0.2$ w/w). Key (○) $T = 165$ °C; (●) $T = 20$ °C. The straight line represents the asymptotic behavior for a wormlike chain. The curved line is a fit with eqs 3 and 4 (see text).

The X-ray diffraction patterns presented in Figure 13 have been recorded for four different polymer fractions at 90 °C to avoid the very intense peak of naphthalene crystals. The intense reflections seen up to $X_{pol} = 0.61$ at $q = 5.5$ and 7.4 nm^{-1} are characteristic peaks for the δ form of sPS. At a polymer fraction $X_{pol} = 0.70$ and $X_{pol} = 0.78$, the reflections at $q = 4.5$, 7.6, 8.6, 9.0, and 10.0 nm^{-1} clearly indicate the overwhelming presence of the β form of sPS, although reflections of the δ form, admittedly rather weak, are still observed. This is consistent with the phase diagram where the conformational change from the 2_1 *helix* to *planar zigzag* is expected to take place as a function of polymer concentration.

These results show that there is no difference, as far as the diffraction pattern is concerned, in the concentration range from $X_{pol} = 0.40$ to $X_{pol} = 0.61$ although the two different compounds C_1 and C_2 are involved. Clearly, the only difference lies in the value of their stoichiometries.

Results of neutron diffraction experiments reported elsewhere[21] confirm the existence of compounds up to a concentration $X_{pol} = 0.78$. Again, this only difference between compound C_1 and compound C_2 lies in the value of the stoichiometry.

Typical curves obtained by small-angle neutron scattering for sPS/Naphthalene at a polymer concentration $X_{pol} = 0.2$ g/cm^3 are drawn in Figure 14. These curves stand for the sPS chain conformation at $T = 20$ °C (solid

state) and at $T = 165$ °C (liquid state). In the liquid state, the scattering curve suggests the existence of a wormlike chain. The calculation of the form factor of such a structure with a finite length L is not straightforward, and so far only semianalytical expressions have been derived by Yoshisaki and Yamakawa[22] and Sharp and Bloomfield.[23] They are as follows:

• For $ql_p \leq 2$

$$P_1(q) = \frac{2}{X}(\exp - X - 1 + X) + \frac{2l_p}{15L}\left[4 + \frac{7}{X} - \left(11 + \frac{7}{X}\right)\exp - X\right] \quad (3)$$

where $X = q^2 l_p L/3$.

• For $2 < ql_p < 4$

$$q^2 l_p L P_2(q) = 6 + 0.547(ql_p)^2 - 0.01569(ql_p)^3 - 0.002816(ql_p)^4 \quad (4)$$

• For $ql_p \gg 1$, the asymptotic behavior as calculated by Des Cloizeaux[24]

$$P_\infty(q) \propto \frac{\pi}{qL} + \frac{2}{3q^2L^2} \quad (5)$$

A fit with these equations gives a persistence length of about $l_p = 2.2$ nm. The mass per unit length determined from the asymptotic behavior is about $\mu_L \approx 500$ g/(nm mol), a value close to that of the 2_1 helical conformation (about 550 g/(nm mol)). In the solid state, the intensity increases significantly at low q while the scattering curves for the solid state and the liquid state merge at high q. These results are reminiscent of those obtained with sPS/benzene[9] and sPS/toluene[10] systems. In the solid state, intermolecular scattering terms are considerably enhanced due to aggregation, which results in an increase of intensity at low q. Conversely, these terms become negligible at high q so that the intensity in this domain reflects the local chain conformation. As in the solid state this conformation is known to be a 2_1 helix, the merging the scattering curves confirms that the chain takes on a similar conformation in the liquid state. These results therefore indicate that the chains are relatively rigid in the liquid state, despite the relatively high temperature within the medium, and is close to the 2_1 helical conformation. On cooling these chains start aggregate but are prevented from folding owing to this rigidity. Eventually, only fibrils can grow instead of chain-folded crystals that would have otherwise given spherulites.

Concluding Remarks

The phase diagrams established by investigation into the thermal behavior of sPS/*trans*-decalin, sPS/tetralin, and sPS/naphthalene indicate the formation of polymer/solvent compounds in all three systems. These outcomes are borne out by X-ray and neutron diffraction experiments. Only the number and the nature of compounds together with the values of stoichiometries depend on the solvent type. It seems that the presence of phenyl rings increase the number of compounds as already observed in the case of benzene where two compounds have been also identified. Removing the "benzene" character of the solvent by protonation, as is the case with tetralin and *trans*-decalin, decreases the number of compounds from two to one but also changes the nature of the compounds. For a totally protonated naphthalene derivative, namely *trans*-decalin, one is dealing with an *incongruently melting* compound unlike what is observed with the partially protonated naphthalene (tetralin) and naphthalene. This might be the reason sPS/*trans*-decalin systems produce spherulitic morphology while sPS/naphthalene and sPS/tetralin systems form fibrillar structures. Helix stabilization, or in other words persistence length enhancement, is thought to be required for growing fibrillar structure instead of chain-folded crystals,[25] something which might depend on the type of compound. In the case of an incongruently melting compound, helix stabilization is likely to be less efficient as the helical form transforms before melting into a more stable conformation, the planar zigzag, which rather produces chain-folded crystals.

Acknowledgment. IFCPAR-CEFIPRA is gratefully acknowledged for the financial support of this work (Grant No. 2808-2). Sudip Malik is also indebted to IFCPAR-CEFIPRA (Grant No. 2808-2) for a postdoctoral fellowship. The authors are also greatly indebted to Bruno Deme for experimental assistance on D16 (ILL, Grenoble, France), and to Annie Brûlet for assistance on PAXE (LLB, Saclay, France). We thank Dr. P. Schultz for the use of the cryofracturing apparatus developed by Dr. J.-C. Homo at the IGBMC UMR 7104 (Illkirch), and C. Straupe for performing the SEM investigations.

References and Notes

(1) Ishihara, N.; Seimiya, T.; Kuramoto, M.; Uoi, M. *Macromolecules* **1986**, *19*, 2465.
(2) Grassi, A.; Pellechia, P.; Longo, P.; Zambelli, A. *Gazz. Chim. Ital.* **1987**, *117*, 249.
(3) Malanga, M. *Adv. Mater.* **2002**, *12*, 1869.
(4) Immirzi, A.; de Candia, F.; Ianelli, P.; Zambelli, A.; Vittoria, V. *Makromol. Chem. Rapid Commun.* **1988**, *9*, 761.
(5) Vittoria, V.; de Candia, F.; Ianelli, P.; Immirzi, A. *Makromol. Chem. Rapid Commun.* **1988**, *9*, 765.
(6) Guerra, G.; Vitagliano, V. M.; De Rosa, C.; Petraccone, V.; Corradini, P. *Macromolecules* **1990**, *23*, 1539.
(7) Chatani, Y.; Shimane, Y.; Inagaki, T.; Ijitsu, T.; Yukinari, T.; Shikuma, H. *Polymer* **1993**, *34*, 1620.
(8) Daniel, C.; Guerra, G. *Soft Mater.* **2004**, *2*, 47.
(9) Daniel, C.; De Luca, M. D.; Brulet, A.; Menelle, A.; Guenet, J. M. *Polymer* **1996**, *37*, 1273.
(10) Daniel, C.; Brulet, A.; Menelle, A.; Guenet, J. M. *Polymer* **1997**, *38*, 4193.
(11) Kobayashi, M. *Macromol. Symp.* **1997**, *114*, 1.
(12) Rudder, J. D.; Berghmans, H.; Schryver, F. C. D.; Basco, M.; Paoletti, S. *Macromolecules* **2002**, *35*, 9529.
(13) Moyses, S.; Sonntag, P.; Spells, S. J.; Laveix, O. *Polymer* **1998**, *39*, 3665.
(14) Ray, B.; Elhasri, S.; Thierry, A.; Marie, P.; Guenet, J. M. *Macromolecules* **2002**, *35*, 9730.
(15) Yoshika, A.; Tashiro, K. *Macromolecules* **2003**, *36*, 3001.
(16) Klein, M.; Menelle, A.; Mathis, A.; Guenet, J.-M. *Macromolecules* **1990**, *23*, 4591.
(17) Point, J. J.; Damman, P.; Guenet, J.-M. *Polym. Commun.* **1991**, *32*, 477.
(18) Cotton, J. P. In *Neutron, X-ray and Light Scattering*; Lindner, P., Zemb, T., Eds.; Elsevier: Amsterdam, 1991.
(19) Deberdt, F.; Berghmans, H. *Polymer* **1993**, *34*, 2192.
(20) Guenet, J. M. *Macromol. Symp.* **2003**, *203*, 1.
(21) Malik, S.; Rochas, C.; Guenet, J. M. *Macromolecules* **2005**, *38*, 4888.
(22) Sharp, P.; Bloomfield, V. A. *Biopolymers* **1968**, *6*, 1201.
(23) Yoshisaki, T.; Yamakawa, H. *Macromolecules* **1980**, *13*, 1518.
(24) Des Cloiseaux, J. *Macromolecules* **1973**, *6*, 403.
(25) Guenet, J. M. *Trends Polym. Sci.* **1996**, *4*, 6.

MA050793F